Finite difference modelling in structurally complex 3D orthorhombic medium

Pavan Elapavuluri and John C. Bancroft

ABSTRACT

Modelling seismic data is a very important aspect in exploration seismology; it is widely used in all the phases of seismic exploration. In this paper, a wave equation for a structurally complex orthorhombic medium is derived and is then used to model data over a thrust sheet model. The data generated is compared to the physical modelling data showing that the traveltimes of both physical modelling data and the numerical data match.

INTRODUCTION

The velocity structure of the earth is fundamentally anisotropic, i.e. the velocity varies with the direction of propagating of energy. Modelling algorithms which are used to model seismic data currently do not take into account the velocity anisotropy. Seismic modelling plays a very important role in exploration seismology. It is used in planning and designing seismic surveys, processing of acquired data and in the interpretation of the data.

Anisotropy is an area of active research as shown by the number of publications over the last few decades. Helbig (e.g. Helbig, 1980), Thomsen (e.g. Thomsen, 1986), Alkhalifah (e.g. Alkhalifah et al., 1996), and Tsvankin (e.g. Tsvankin and Thomsen, 1994) have published many papers on the topic of anisotropy. Alkhalifah (2000) derived a wave equation for acoustic medium in the paper titled "Acoustic wave equation for VTI medium." Later, he proposed a scheme for numerically modelling seismic data in orthorhombic medium (Alkhalifah, 2003). Zhang et al. (2002) extended Alkhalifah's VTI formulation to TTI medium.

The most common symmetry observed in the context of exploration seismology, is Vertical Transverse Isotropy (VTI). VTI symmetry, as the name implies, is only valid when the symmetry axis is vertical. The approximation of VTI symmetry is not valid when the axis of symmetry is tilted, such as in structurally complex areas. The case in which the axis of symmetry is not vertical is termed tilted transverse isotropy (TTI). Most of the commercial seismic modelling programs that are available, like *NORSAR* and *GX II*, simulate VTI medium, but can't handle TTI medium. A more generalized medium with two axes of symmetry is orthorhombic medium. In this paper we propose a technique to model seismic data in structurally complex orthorhombic media.

ORTHORHOMBIC MEDIUM

Orthorhombic media, unlike VTI media has three mutually orthogonal planes of mirror symmetry Tsvankin (2001); nine independent stiffness coefficients are needed to describe this symmetry.

The most common example of orthorhombic symmetry in real geology is that of sedimentary basins in a combination of parallel vertical fractures with vertical transverse sym-

metry in the background. Bakulin et al. (2000) states that orthorhombic symmetry may be the simplest realistic symmetry for many geophysical problems. This symmetry is illustrated in Figure 1.

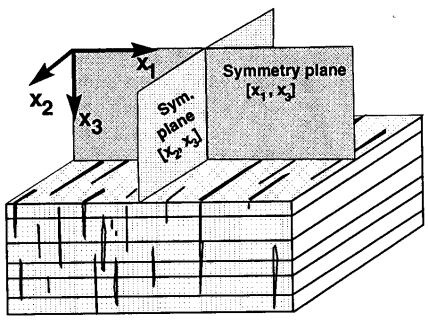

FIG. 1. Orthorhombic symmetry. Courtesy (Tsvankin, 2001)

Stiffness matrix for Orthorhombic medium

The Christoffel equation for a orthorhombic media can written as follows:

$$c_{ij} = \begin{pmatrix} c_{11} & c_{12} & c_{13} & 0 & 0 & 0 \\ c_{12} & c_{22} & c_{23} & 0 & 0 & 0 \\ c_{13} & c_{23} & c_{33} & 0 & 0 & 0 \\ 0 & 0 & 0 & c_{44} & 0 & 0 \\ 0 & 0 & 0 & 0 & c_{55} & 0 \\ 0 & 0 & 0 & 0 & 0 & c_{66} \end{pmatrix}, \tag{1}$$

where c_{ij} are the Christoffel's coefficients, which are related to the velocities a_{ij} by

$$A_{ij} = c_{ij}/\gamma, \tag{2}$$

where γ is the density. The Christoffel's matrix shown in Equation 1 has nine independent coefficients. This equation reduces to that of an equation in VTI media in the degenerate case.

Anisotropy parameters in orthorhombic media

Tsvankin (2001) has introduced anisotropic parameters that characterize a wide range of signatures for orthorhombic anisotropy. He used the orthorhombic anisotropy's analogy with VTI media to propose these parameters on the lines of Thomsen's parameters for VTI media.

There are *five* independent parameters which can be used to classify this media, they are: $\epsilon^{(2)}$, $\delta^{(2)}$, $\epsilon^{(1)}$, $\delta^{(1)}$ and $\delta^{(3)}$.

The subscript refers to the normal direction of the symmetry axis; for example the subscript(2) refers to the x_2 axis, which defines the normal direction to the $[x_1, x_3]$ symmetry

plane. $\epsilon^{(2)}$ be written as:

$$\epsilon^{(2)} = \frac{c_{11} - c_{33}}{2c_{33}} \tag{3}$$

$\delta^{(2)}$ be written as

$$\delta^{(2)} = \frac{(c_{13} + c_{55})^2 - (c_{33} - c_{55})^2}{2c_{33}(c_{33} - c_{55})} \tag{4}$$

It can be easily noted that $\epsilon^{(2)}$ and $\delta^{(2)}$ are analogous to the parameters ϵ and δ in VTI media. The only difference is the coefficient c_{44} is used to calculate δ in VTI media, while in orthorhombic media the coefficient c_{55} is used. The parameters in the $[x_2, x_3]$ symmetry plane can be written as:

$$\epsilon^{(1)} = \frac{c_{22} - c_{33}}{c_{33}}, \tag{5}$$

and $\delta^{(1)}$ can be written as

$$\delta^{(1)} = \frac{(c_{23} + c_{44})^2 - (c_{33} - c_{44})^2}{2c_{33}(c_{33} - c_{44})}. \tag{6}$$

The above four anisotropy parameters can be used to calculate the eight stiffness coefficients: $c_{11}, c_{22}, c_{33}, c_{44}, c_{55}, c_{66}, c_{23}$ and c_{13}. The only remaining stiffness c_{12} can be replaced with a dimensionless anisotropic parameter $\delta^{(3)}$ analogous to the coefficients $\delta^{(1)}$ and $\delta^{(2)}$:

$$\delta^{(3)} = \frac{(c_{12} + c_{66})^2 - (c_{11} - c_{66})^2}{2c_{11}(c_{11} - c_{66})}. \tag{7}$$

THEORY

The main objective of this paper is to develop a modelling algorithm which can be used to model 3-D seismic data in structurally complex anisotropic medium. This modelling technique will be implemented using a Finite Difference technique.

In order to derive the wave equation in TTI medium, we first examine the formulation for phase velocity orthorhombic medium Daley et al. (1999).

WAVE EQUATION IN ORTHORHOMBIC MEDIA

The wave equation in orthorhombic medium can be written as equation 8. This equation is derived in Appendix A.

$$\begin{aligned}\frac{\partial \psi}{\partial t^2} = (A_{11}\frac{\partial^2}{\partial x^2} + A_{22}\frac{\partial^2}{\partial y^2} + A_{33}\frac{\partial^2}{\partial z^2} + \\ B_{12}\frac{\partial^2}{\partial x \partial y} + B_{23}\frac{\partial^2}{\partial y \partial z} + \\ B_{13}\frac{\partial^2}{\partial x \partial z})\psi\end{aligned} \tag{8}$$

where $B_{12} = 2(A_{12} + 2A_{66})B_{23} = 2(A_{23} + 2A_{44})$ and $B_{13} = 2(A_{13} + 2A_{55}$ The equation (8) is the wave equation in Orthorhombic media. This equation can be solved using various

techniques to model the data; in this paper, this equation is the solved using finite difference method.

This equation is valid in flat layered orthorhombic medium. If the media were structurally complex, we need to transform this wave equation to be valid in structurally complex medium. The following method is used to achieve this transformation.

AXIS ROTATION IN 3-D ORTHORHOMBIC MEDIA

Up to this point we have defined the velocities, A_{11},A_{22}, A_{33}, B_{13}, B_{12}, B_{23}, with respect to the principal crystallographic axis. Therefore, for structurally deformed medium, we need to rotate the system through the deformation angle. In a 2D system this rotation from unrotated (primed) system to the rotated (un primed) system can be implemented using the following scheme (Daley et al., 1999):

$$\begin{bmatrix} x \\ z \end{bmatrix} = \begin{bmatrix} \cos(\theta) & -sin(\theta) \\ \sin(\theta) & cos(\theta) \end{bmatrix} \begin{bmatrix} x\prime \\ z\prime \end{bmatrix}. \tag{9}$$

Using the above orthogonal matrix, the unrotated directional space derivatives can be written in rotated coordinates as follows:

$$\frac{\partial}{\partial x} = \cos\theta \frac{\partial}{\partial x\prime} - \sin\theta \frac{\partial}{\partial z\prime} \tag{10}$$

and

$$\frac{\partial}{\partial z} = \sin\theta \frac{\partial}{\partial x\prime} + \cos\theta \frac{\partial}{\partial z\prime}. \tag{11}$$

Now we will generalize this rotation scheme to 3D media.

Rotation Matrices in 3D media

Rotation matrix is a matrix corresponding to a rotation of a set of points around a certain axis, through some arbitrary angle θ. Rotations can be represented by orthogonal matrices, a matrix $\mathbf{A}$ is said to orthogonal when $\mathbf{A}\mathbf{A}^{\mathbf{T}} = \mathbf{1}$. In 3D, the rotation about $x-$ axis is given by:

$$\begin{bmatrix} 1 & 0 & 0 \\ 0 & \cos\theta & -\sin\theta \\ 0 & \sin\theta & \cos\theta \end{bmatrix}, \tag{12}$$

the rotation about $y-$axis is given by:

$$\begin{bmatrix} \cos\theta & 0 & \sin\theta \\ 0 & 1 & 0 \\ -\sin\theta & 0 & \cos\theta \end{bmatrix}, \tag{13}$$

and the rotation about $z-$axis is given by:

$$\begin{bmatrix} \cos\theta & -\sin\theta & 0 \\ \sin\theta & \cos\theta & 0 \\ 0 & 0 & 1 \end{bmatrix}. \tag{14}$$

Rotation scheme in generalized 3D media

Orthorhombic media, in contrast to VTI and Horizontal Transverse Isotropy (HTI) , which have only one axis of symmetry, has two axes of symmetry. The rotation scheme can be easily explained by taking the example of 2D VTI media. Suppose we can transform this media into a TTI media by using the transformation using the equation (9). Being a 2D rotation, it is not necessary to specify the axis on which it is to be rotated. Now consider a 3D VTI media to be transformed into a TTI media, the question arises, along which axis should the media need to be rotated? The answer to this question depends on how the velocity model is being setup. If the strike of the model is along the $x-$ axis then the dip is nothing but rotation along the $y-$axis and the azimuth would be the rotation along the $z-$ axis. Therefore the the whole 3D rotation can be written as this matrix:

$$\begin{bmatrix} x \\ y \\ z \end{bmatrix} = \begin{bmatrix} 1 & 0 & 0 \\ 0 & \cos\theta & -\sin\theta \\ 0 & \sin\theta & \cos\theta \end{bmatrix} \begin{bmatrix} \cos\theta & 0 & \sin\theta \\ 0 & 1 & 0 \\ -\sin\theta & 0 & \cos\theta \end{bmatrix} \begin{bmatrix} \cos\theta & -\sin\theta & 0 \\ \sin\theta & \cos\theta & 0 \\ 0 & 0 & 1 \end{bmatrix} \begin{bmatrix} x\prime \\ y\prime \\ z\prime \end{bmatrix} \tag{15}$$

Properties of rotation matrix

The following are the properties of rotation matrices:

- Rotational matrices are not commutative therefore the order in which they are applied is very important
- Rotational matrices are orthogonal matrices

Considering the non-commutative nature of these matrices, care should be taken on how the rotational matrices are applied.

Rotation scheme in orthorhombic media

For simplicity's sake let us considering only 2.5D media, with strike along the $x-$axis; therefore rotation for the dip should be along the $y-$axis; this rotation would transform the background VTI symmetry to tilted transverse isotropy (TTI) symmetry. This being orthorhombic media there is an other axis of symmetry which should be rotated. This axis of symmetry is usually due to the presence of fractures perpendicular to the strike of the model (Tsvankin, 2001). In structurally complex orthorhombic media the rotation of orientation of these fractures can be treated as a rotation along the $z-$axis.

Order of rotation

We follow a convention of applying rotation is across the $y-$axis first, rotating the VTI symmetry into TTI. The second rotation is then applied along the $z-$axis, rotating the orientation of the fractures. This being a 2.5D media there is no rotation across the azimuth.

The final rotation matrix can be written as:

$$\begin{bmatrix} x \\ y \\ z \end{bmatrix} = \begin{bmatrix} 1 & 0 & 0 \\ 0 & \cos\theta & -\sin\theta \\ 0 & \sin\theta & \cos\theta \end{bmatrix} \begin{bmatrix} 1 & 0 & 0 \\ 0 & \cos\theta & -\sin\theta \\ 0 & \sin\theta & \cos\theta \end{bmatrix} \begin{bmatrix} x\prime \\ y\prime \\ z\prime \end{bmatrix} \tag{16}$$

Equation (16) is solved for the slownesses in x, y and z rotations and substituted in the wave equation (equation (8)); this equation is then solved using a fourth order finite difference scheme to generate the numerical seismic data.

This equation is now tested on different models.

TESTING

This finite difference modelling algorithm is then tested on various homogeneous models with various anisotropy parameters and various orientations of axes of symmetry.

Model 1

The model 1 parameters are

- Velocity=3755 m/s
- $\epsilon^{(2)}$=0.2
- $\delta^{(2)}$=0.2
- $\epsilon^{(1)}$=0.2
- $\delta^{(1)}$=0.2
- $\delta^{(3)}$=0.2

A snapshot of the wave propagating is shown in Figure 2. The shot is located at the centre of the model.

Model 2

The model 2 parameters are

- Velocity=3755 m/s
- $\epsilon^{(2)}$=0.2
- $\delta^{(2)}$=0.1
- $\epsilon^{(1)}$=0.2
- $\delta^{(1)}$=0.1

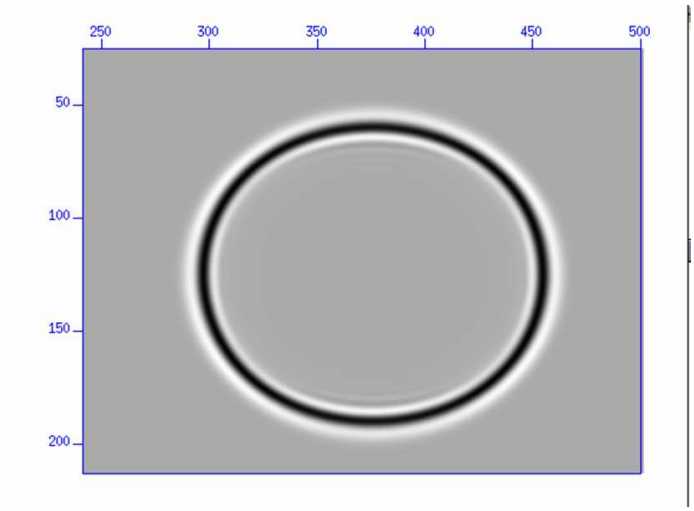

FIG. 2. Snapshot of the wavefront in model 1.

- $\delta^{(3)}$=0.1

A snapshot of the wave propagating is shown in Figure 3. The shot is located at the centre of the model.

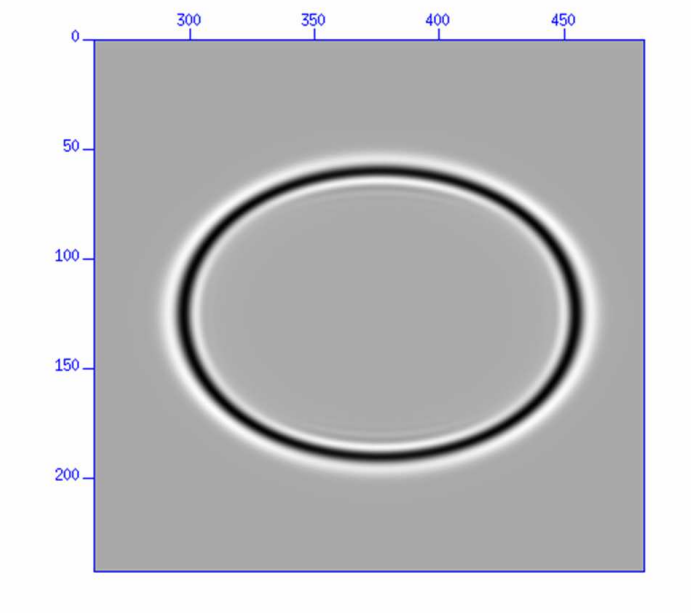

FIG. 3. Snapshot of the wavefront in model 2.

Model 3

The model 3 parameters are

- Velocity=3755 m/s

- $\epsilon^{(2)}$=0.2
- $\delta^{(2)}$=-0.2
- $\epsilon^{(1)}$=0.2
- $\delta^{(1)}$=-0.2
- $\delta^{(3)}$=-0.2

A snapshot of the wave propagating is shown in Figure 4. The shot is located at the centre of the model.

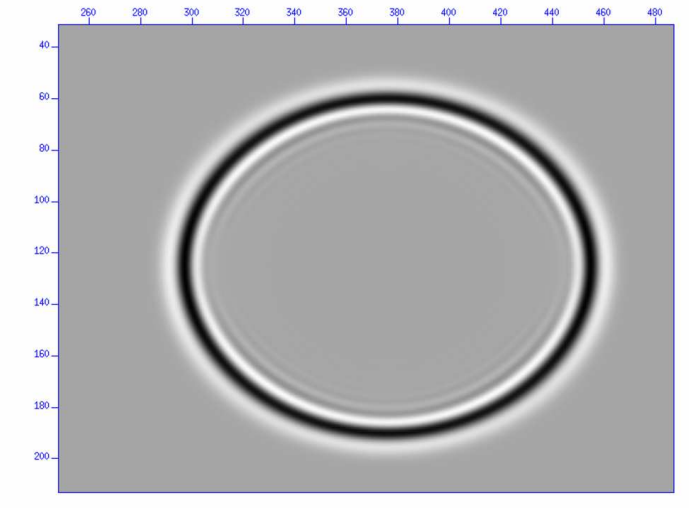

FIG. 4. Snapshot of the wavefront in model 3.

Model 4

The model 4 parameters are

- Velocity=3755 m/s
- dip=15°
- fracture orientation=10°
- $\epsilon^{(2)}$=0.2
- $\delta^{(2)}$=-0.2
- $\epsilon^{(1)}$=0.2
- $\delta^{(1)}$=-0.2
- $\delta^{(3)}$=-0.2

A snapshot of the wave propagating is shown in Figure 5. The shot is located at the centre of the model.

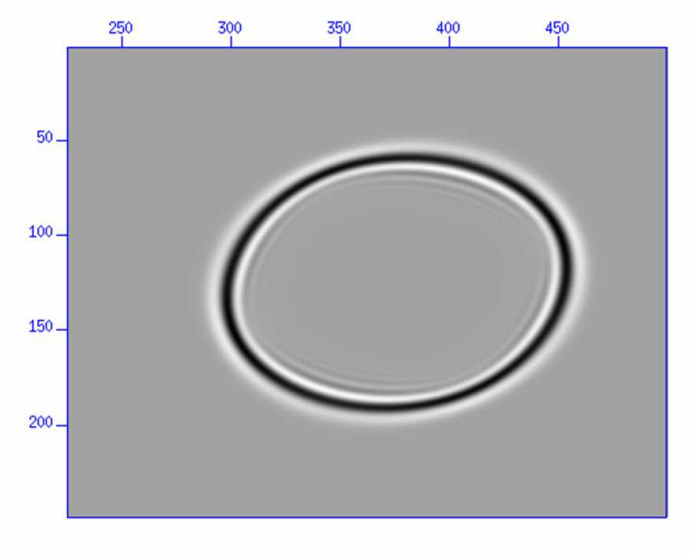

FIG. 5. Snapshot of the wavefront in model 4.

Model 5

The model 5 parameters are

- Velocity=3755 m/s
- dip=30°
- fracture orientation=10°
- $\epsilon^{(2)}$=0.2
- $\delta^{(2)}$=-0.2
- $\epsilon^{(1)}$=0.2
- $\delta^{(1)}$=-0.2
- $\delta^{(3)}$=-0.2

A snapshot of the wave propagating is shown in Figure 6. The shot is located at the centre of the model.

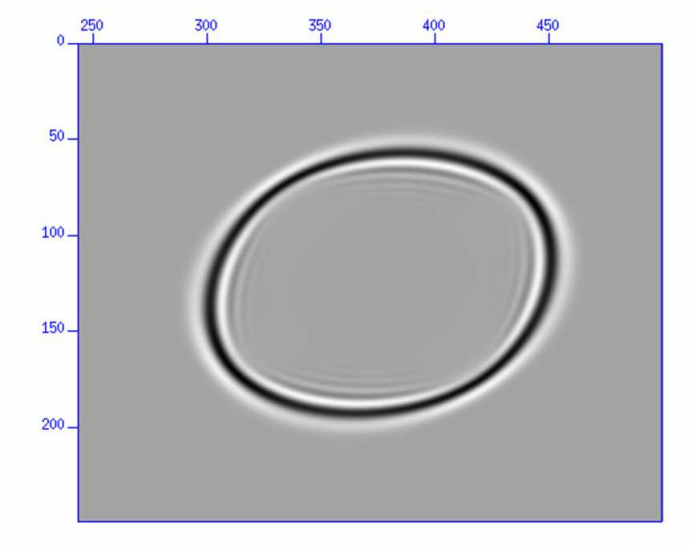

FIG. 6. Snapshot of the wavefront in Model 5.

Model 6

The model 6 parameters are

- Velocity=3755 m/s
- dip=45°
- fracture orientation=10°
- $\epsilon^{(2)}$=0.2
- $\delta^{(2)}$=-0.2
- $\epsilon^{(1)}$=0.2
- $\delta^{(1)}$=-0.2
- $\delta^{(3)}$=-0.2

A snapshot of the wave propagating is shown in Figure 7. The shot is located at the centre of the model.

Model 7

The model 7 parameters are

- Velocity=3755 m/s
- dip=60°

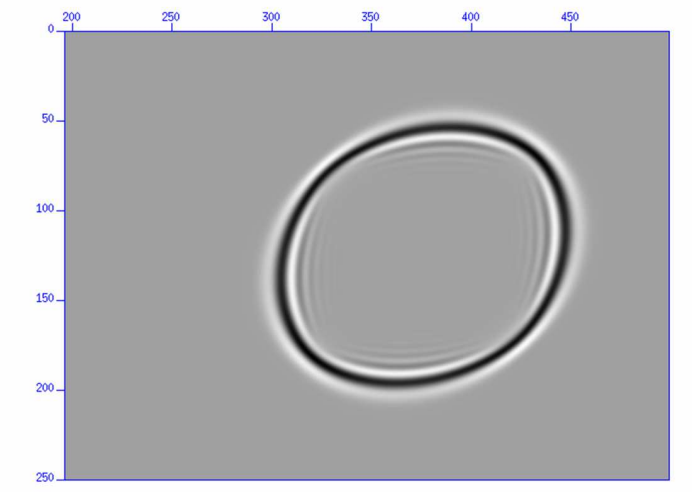

FIG. 7. Snapshot of the wavefront in medium Model 6.

- fracture orientation=10°
- $\epsilon^{(2)}$=0.2
- $\delta^{(2)}$=-0.2
- $\epsilon^{(1)}$=0.2
- $\delta^{(1)}$=-0.2
- $\delta^{(3)}$=-0.2

A snapshot of the wave propagating is shown in Figure 8. The shot is located at the centre of the model.

THRUST SHEET MODEL

Leslie and Lawton (2001) acquired seismic data over a physical model of an anisotropic thrust sheet. The physical model is illustrated in Figure 9. The algorithm described above is now tested on this model.

Comparison between numerical and physical modelling data

Figure 10 allows for the comparison at the shot records acquired over the physical modelling data and the numerical modelling data. It can be seen that the traveltimes in both sections match with each other (Figure 10). The interesting section in the data is where the dipping anisotropic section meets the surface. As the anisotropic layer's fast direction is oriented up wards towards the surface, a pull up in traveltime is expected. We see a pull up in traveltime of the same magnitude in both the physical model data and the numerical model data.

The energy below the main reflection in the numerical modelling data is due to edge reflections.

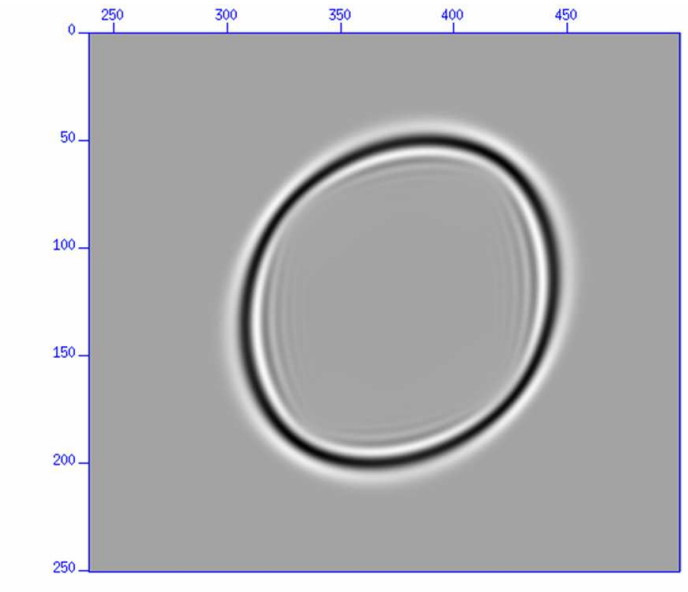

FIG. 8. Snapshot of the wavefront in medium model 7.

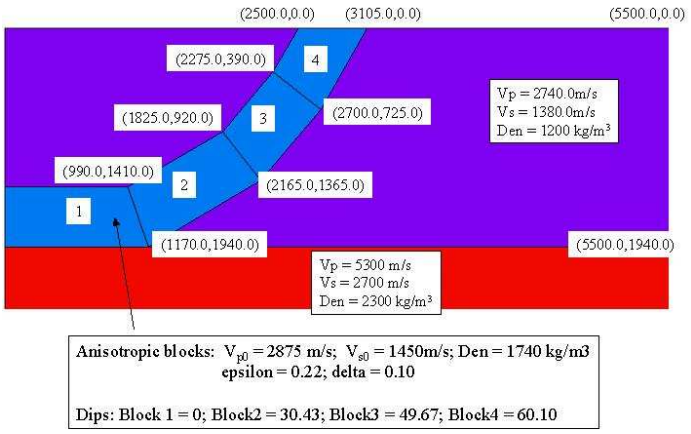

FIG. 9. Thrust sheet model (Courtesy Don Lawton).

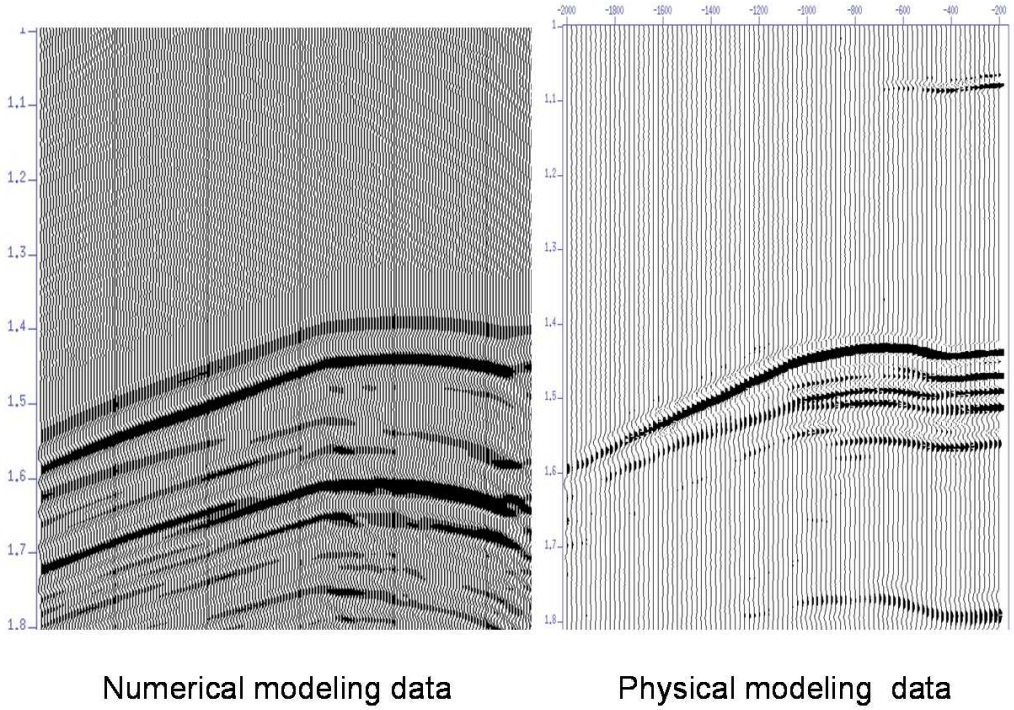

FIG. 10. Comparison between numerical modelling data and physical modelling data.

Comparison between numerical and physical modelling data

Figure 10 allows for the comparison at the shot records acquired over the physical modelling data and the numerical modelling data.

It can be seen that the traveltimes in both sections match with each other (Figure 10). The interesting section in the data is where the dipping anisotropic section meets the surface. As the anisotropic layer's fast direction is oriented upwards towards the surface, a pull up in traveltime is expected. We see a pull up in traveltime of the same magnitude in both the physical model data and the numerical model data.

The energy below the main reflection in the numerical modelling data is due to edge reflections.

CONCLUSIONS

In this paper we derived a wave equation for a TTI medium. We tested this equation on various simple models and displayed snapshots. The algorithm is then applied to a numerical version of a thrust sheet model. The data is then compared to the data acquired on a physical version of the same model. In future, we plan to extend this method to 3-D medium, and to improve the boundary condition implementation in the modelling code.

ACKNOWLEDGEMENTS

Dr. Don Lawton is thanked for providing the physical modelling data. We also acknowledge Gary Billings of Talisman Energy and Pat Daley of CREWES for all their help.

The CREWES sponsors are thanked for their continued support.

REFERENCES

Alkhalifah, T., 2000, An acoustic wave equation for anisotropic media: Geophysics, **65**, No. 4, 1239–1250.

Alkhalifah, T., 2003, An acoustic wave equation for orthorhombic anisotropy, **68**, No. 4, 1169–1172.

Alkhalifah, T., Tsvankin, I., Larner, K., and Toldi, J., 1996, Velocity analysis and imaging in transversely isotropic media: Methodology and a case study: The Leading Edge, **15**, No. 05, 371–378.

Bakulin, A., Grechka, V., and Tsvankin, I., 2000, Estimation of fracture parameters from reflection seismic data – Part I: HTI model due to a single fracture set: Geophysics, **65**, No. 6, 1788–1802.

Daley, P. F., 2005, Basic pseudo-differential operator theory in a transversely isotropic medium for qP wave propogation: Personal Communication.

Daley, P. F., Marfurt, K. J., and McCarron, E. B., 1999, Finite-element ray tracing through structurally deformed transversely isotropic formations: Geophysics, **64**, No. 3, 954–962.

Helbig, K., 1980, Modeling of transversely isotropic media by thin isotropic layers, *in* 50th Ann. Internat. Mtg, Soc. of Expl. Geophys., Session:R.30.

Leslie, J. M., and Lawton, D. C., 2001, P-wave traveltime anomalies below a dipping anisotropic thrust sheet, *in* Advances, Soc. of Expl. Geophys., 77–84.

Thomsen, L., 1986, Weak elastic anisotropy: Geophysics, **51**, No. 10, 1954–1966.

Tsvankin, I., 2001, Seismic Signatures and Analysis of Reflection Data in Anisotropic Media: Pergamon.

Tsvankin, I., and Thomsen, L., 1994, Nonhyperbolic reflection moveout in anisotropic media: Geophysics, **59**, No. 08, 1290–1304.

Zhang, L., Rector, J., and Hoversten, G., 2002, An Eikonal solver in tilted TI media, *in* 71st Ann. Internat. Mtg, Soc. of Expl. Geophys., 1955–1958.

APPENDIX A

In this section we derive the wave equation in orthorhombic medium; this derivation is based on (Daley, 2005). The linearized quasi-compressional (QA) Eikonal in transversely isotropic medium can be written as:

$$G_{PP}(x_k, P_k) = A_{11}P_1^2 + A_{33}P_3^2 + \frac{B_{13}P_1^2P_3^2}{P_1^2 + P_3^2} = 1 \tag{A-1}$$

where

$$B_{13} = 2(A_{13} + 2A_{55}) - (A_{11} + A_{33}). \tag{A-2}$$

Now let us assume a solution of the form:

$$Amplitude\ potential \propto \exp^{-i\omega t + K_1 x_1 + I_3 x_3}, \tag{A-3}$$

the pseudo-differential operators, with $IL_1 = i\omega p_1$ and $ink_3 = i\omega p_3$ can be written as:

$$\begin{aligned} -i\omega &\rightarrow \frac{\partial}{\partial t} \\ -ilk_1 &\rightarrow \frac{\partial}{\partial x_1} \\ -Ki_3 &\rightarrow \frac{\partial}{\partial x_3}. \end{aligned} \tag{A-4}$$

Now rewriting equation A-1 in symmetric operator notation, for some operation "o" as:

$$p_1^2 A_{11} p_1^2 + p_3^2 A_{33} p_1^3 + p_1 p_3 B_{13} p_1 p_3 - (p_1 A_{00} p_1 + p_3 A_{00} p_3) o = 0, \tag{A-5}$$

where $B_{13} = 2(A_{13} + 2A_{55})$ and for convenience a quantity $A_{00} \equiv \forall[\mathbf{x} : (-\infty < \mathbf{x} > \infty)]$ has been introduced. The partial derivative operations defined in equation A-4 are introduced by first multiplying equation A-5 by $i\omega^4$. It is assumed that equation A-5 operates on some function (potential) ϕ such that some force is defined by $\mathbf{u} = \boldsymbol{\Delta}\phi$ and the resultant pressure is given by $P = \Delta.\Delta\phi = \Delta.\mathbf{u} = \boldsymbol{\Delta}^{\mathbf{2}}\phi$ to obtain

$$\partial_1^2(A_{11}\partial_1^2\phi) + \partial_3^2(A_{33}\partial_3^2\phi) + \partial_1\partial_3(B_{13}\partial_1\partial_3\phi) - \partial_t^2(\partial_1^2 + \partial_3^2)\phi = 0 \tag{A-6}$$

The above equation is the most general case, as it assumes that the anisotropic parameters A_j are spatial dependent, i.e., $A_i \equiv A_J(x_1, x_3)$. It is often convenient to write a part of equation A-6 in terms of pressure so that equation A-6 becomes

$$\partial_1^2(A_{11}\partial_1^2\phi) + \partial_3^2(A_{33}\partial_3^2\phi) + \partial_1\partial_3(B_{13}\partial_1\partial_3\phi) - \partial_t^2 P = 0 \tag{A-7}$$

Equation A-7 is a wave equation in VTI media, and using the same analysis the equation in orthorhombic media can be written as

$$\begin{aligned} &\partial_1^2(A_{11}\partial_1^2\phi) + \partial_2^2(A_{22}\partial_2^2\phi) + \partial_3^2(A_{33}\partial_3^2\phi) \\ &+\partial_1\partial_3(B_{13}\partial_1\partial_3\phi) + \partial_1\partial_2(B_{12}\partial_1\partial_2\phi) + \partial_2\partial_3(B_{23}\partial_2\partial_3\phi) - \partial_t^2 P = 0 \end{aligned} \tag{A-8}$$